

Tunnelling induced collapse of an atomic Bose-Einstein condensate in a double-well potential

E. Sakellari, N.P. Proukakis and C.S. Adams

Department of Physics, University of Durham, South Road, Durham DH1 3LE,
United Kingdom

E-mail: n.p.proukakis@durham.ac.uk

Abstract.

The stability of a low temperature Bose-Einstein condensate with attractive interactions in one and three dimensional double-well potentials is discussed. In particular, the tunnelling dynamics of a condensate under the influence of a time-dependent potential gradient is investigated. The condensate is shown to collapse at a critical potential gradient which corresponds to a critical number of atoms in one of the two wells. The sensitivity of this tunnelling induced collapse could provide a useful tool in the study of condensates with attractive interactions.

PACS numbers: 03.75.Lm, 03.75.kk

1. Introduction

The experimental realization of Bose-Einstein condensation (BEC) in dilute atomic gases of ^{87}Rb [1], ^{23}Na [2], ^7Li [3], ^1H [4], metastable ^4He [5], ^{85}Rb [6], ^{41}K [7], ^{133}Cs [8] and ^{174}Yb [9] has stimulated theoretical studies of the properties of ultracold Bose gases. The densities of such systems are typically sufficiently low, that their interactions can be described by a single parameter, the s -wave scattering length a . In addition one can control not only the strength of these interactions but also whether they are attractive ($a < 0$ e.g. ^7Li , ^{85}Rb , ^{133}Cs at low magnetic fields) or repulsive ($a > 0$) using magnetic-field induced Feshbach resonances [10]. Whereas a harmonically confined BEC with repulsive interactions is stable for any number of atoms, a condensate with attractive interactions is only stable if the atom number \mathcal{N} is smaller than a critical value \mathcal{N}_{cr} [3, 11, 12, 13, 14, 15, 16, 17, 18]. For $\mathcal{N} > \mathcal{N}_{\text{cr}}$ the interaction energy exceeds the zero-point kinetic energy and a collapse occurs, as extensively studied in [19, 20, 21, 22, 23, 24, 25, 26, 27, 28]. In experiments on ^7Li , the magnetic field is held fixed and the number of condensate atoms grows up to \mathcal{N}_{cr} where a partial collapse occurs [29, 30]. In this system, it should be noted that the attractive interactions can lead to the formation of bright matter-wave soliton trains in elongated optical traps [31]. In contrast to the ^7Li experiments, in the case of ^{85}Rb , a Feshbach resonance [6] has been used to switch the scattering length from positive to negative values, producing a condensate with $\mathcal{N} \gg \mathcal{N}_{\text{cr}}$ which subsequently collapses [32], as modelled in [33, 34, 35, 36, 37, 38, 39].

Although much work has been done to study the collapse properties of dilute BECs in a single-harmonic trap, an interesting subject is the behaviour of a condensate with attractive interactions in a double-well potential. Magnetic [41, 42] and optical [43, 44] double-well potentials have been created in recent experiments and a proposal for a magnetic double-well has been reported [45]. Although condensates with $a > 0$ in a double-well system have received considerable theoretical attention [46, 47, 48, 49, 50, 51, 52, 53, 54]), only Adhikari [55] and Couillet *et al.* [56] have studied the $a < 0$ case.

In this paper, we investigate the stability of a low temperature atomic condensate with attractive interactions in a double-well potential, where the Josephson dynamics are induced by the addition of a time-dependent potential gradient. Our analysis is based on the Gross-Pitaevskii equation. The aim is to discuss the stability of the condensate in the double-well potential and show how tunnelling between the wells can lead to collapse. We do not, however, intend to describe the *collapse dynamics*, for which, one should at least additionally incorporate a suitable 3-body loss term [36, 40].

Section 2 introduces the main formalism and briefly reviews the eigenenergies of the double-well potential as a function of the potential gradient in both one and three dimensions. Section 3 discusses the stability of a BEC in a three dimensional symmetric double-well as a function of the barrier height. Finally, Section 4 considers the time-dependent evolution of a 3D system as the gradient is increased at a constant rate. We find that a collapse occurs as the gradient is increased above a critical value, which,

within our formalism, can be predicted by the eigenstate curves.

2. Eigenenergy levels of a BEC in a double-well potential

At low temperatures, the condensate wavefunction $\psi(\mathbf{r}, t)$ (normalized to unity) obeys the dimensionless Gross-Pitaevskii (GP) equation,

$$i \frac{\partial}{\partial t} \psi(\mathbf{r}, t) = \left[-\frac{1}{2} \nabla^2 + V(\mathbf{r}) + g_{3D} |\psi(\mathbf{r}, t)|^2 \right] \psi(\mathbf{r}, t). \quad (1)$$

In the above equation, $V(\mathbf{r})$ is the confining potential and $g_{3D} = g/(a_{\perp}^3 \hbar \omega_{\perp})$, is the dimensionless effective interaction term, where $g = \mathcal{N}(4\pi \hbar^2 a/m)$ is the usual three-dimensional scattering amplitude, defined in terms of the s -wave scattering length a , the total number \mathcal{N} of atoms of mass m , and the harmonic oscillator length in the transverse direction(s) $a_{\perp} = \sqrt{\hbar/m\omega_{\perp}}$, with ω_{\perp} the corresponding trapping frequency. The confining potential,

$$V(\mathbf{r}) = \frac{1}{2} (\rho^2 + \lambda^2 z^2) + h \exp(-z^2) + \delta z. \quad (2)$$

describes an axially symmetric potential, with $\rho^2 = x^2 + y^2$ and asymmetry parameter $\lambda = \omega_z/\omega_{\perp}$ plus a Gaussian potential of height h , located at $z = 0$. In addition, a linear potential δz of gradient δ is pivoted at the centre of the trap. For $\delta > 0$, the right well has higher potential energy and the trap centre is additionally shifted into the $z > 0$ region; however, this shift is negligible for the parameters studied throughout this work. Throughout this paper we work in dimensionless (harmonic oscillator) units, by applying the following scalings: space coordinates transform according to $\mathbf{r}'_i = a_{\perp}^{-1} \mathbf{r}_i$, time $t' = \omega_{\perp} t$, condensate wavefunction $\psi'(\mathbf{r}', t') = \sqrt{a_{\perp}^3} \psi(\mathbf{r}, t)$ and energy $E' = (\hbar \omega_{\perp})^{-1} E$ (primes henceforth neglected for convenience).

We can also consider the 1D form of Eq. (1), which accurately takes into account the transverse dynamics of ‘cigar’ condensates ($\lambda < 1$),

$$i \frac{\partial}{\partial t} \psi(z, t) = \left[-\frac{1}{2} \frac{\partial^2}{\partial z^2} + V_{1D}(z) + g_{1D} |\psi(z, t)|^2 \right] \psi(z, t), \quad (3)$$

where $\psi(z)$ is normalized to unity, $g_{1D} = g_{3D}/(2\pi a_{\perp}^2)$ is the 1D self-interaction parameter that matches the 1D and 3D axial density profiles and $V_{1D}(z)$ is the confining potential in the axial direction.

$$V_{1D}(z) = \frac{1}{2} z^2 + h \exp(-z^2) + \delta z. \quad (4)$$

The eigenstates of the double-well condensate in 1D and 3D are calculated by substituting $\psi(\mathbf{r}, t) = e^{-i\mu t} \Psi(\mathbf{r})$, where μ is the chemical potential (of the one and three dimensional system respectively), and solving the resulting time-independent equation as discussed in [53]. For small nonlinearities there are only two levels and, for $\delta = 0$, the eigenstates are a symmetric ground state Ψ_g and an antisymmetric first excited state, Ψ_e , with equal population in both wells. Sufficiently large interactions lead to the appearance of a loop structure (see e.g. [50, 57]). This loop structure appears in

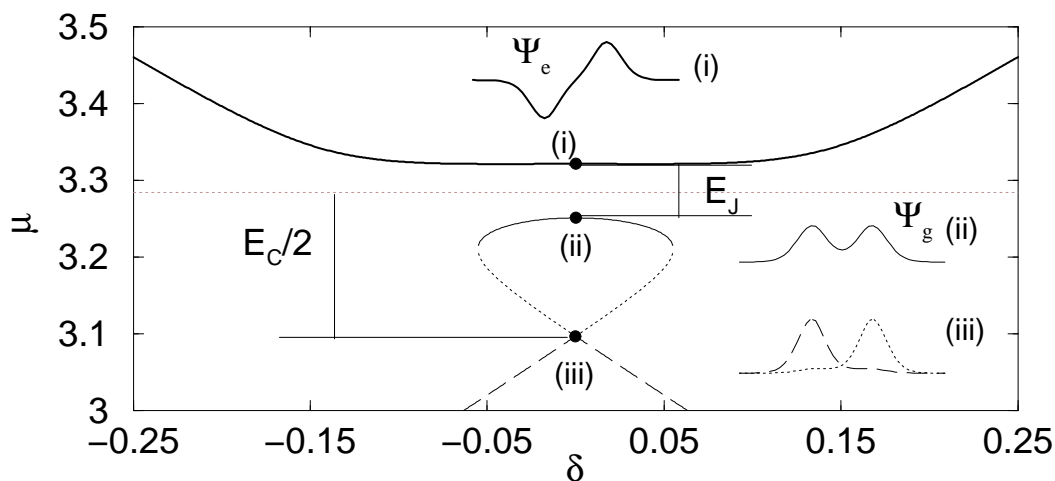


Figure 1. Eigenenergies μ ($\hbar\omega_{\perp}$) for the double-well for an attractive Bose gas as a function of the potential gradient δ ($\hbar\omega_{\perp}/a_{\perp}$) indicating the self-interaction energy, E_C , and the Josephson coupling energy, E_J in each case. The horizontal dotted grey line corresponds to the zero energy of the two-state model. The value of the nonlinearity used here is $g_{3D} = -\pi$, corresponding to $E_C = -0.379\hbar\omega_{\perp}$ and $E_J = 0.071\hbar\omega_{\perp}$. The eigenstates at the centre of the trap are also shown in each case. We assume a spherical trap geometry ($\lambda = 1$), and a Gaussian barrier of height $h = 4\hbar\omega_{\perp}$ located at the centre of the trap.

the first excited state for $a > 0$, and in the ground state for $a < 0$. In this paper we consider the latter case (Fig. 1), for which the corresponding wavefunctions at $\delta = 0$ are: (i) a symmetric ground state Ψ_g with equal population in both wells, (ii) an anti-symmetric state with equal population in both wells and a phase difference of π across the trap centre, which we shall henceforth refer to as Ψ_e , and (iii) two lower energy, non-symmetric ground state solutions with most of the particles in either the left (dashed) or the right (dotted) well (the so-called ‘self-trapped’ states [47, 48, 53, 54]).

Under certain conditions, the eigenenergies μ can also be reproduced by the two-state model (see e.g. [46, 47, 48, 49, 50]) described by the Hamiltonian,

$$H = \frac{1}{2} \begin{pmatrix} -\Delta + E_C N & -E_J \\ -E_J & \Delta - E_C N \end{pmatrix}, \quad (5)$$

where $N = (N_{\ell} - N_r)/\mathcal{N}$ is the fractional population difference, Δ is the potential energy difference between the left (ℓ) and right (r) wells, $E_C = g\langle\Psi_{\ell,r}||\Psi_{\ell,r}|^2|\Psi_{\ell,r}\rangle$ is the self-interaction energy, g is the nonlinearity and $E_J = -2\langle\Psi_{\ell}||(-\frac{1}{2}\nabla^2 + V_{\delta=0})|\Psi_r\rangle$ is the Josephson coupling energy. The energy splittings E_C and E_J are indicated in Fig. 1. For the case of a potential gradient δ , we can write $\Delta = \alpha\delta$, where α is a numerical factor determined numerically from the GP solution. The picture for the eigenenergy levels as a function of δ shown in Fig. 1, is only valid in 1D and 3D for a range of nonlinearities.

Focusing first on the 1D case, we plot in Fig. 2(a) the two-state model parameters $|E_C|$ and E_J at $\delta = 0$ (symmetric double-well) as a function of g_{1D} . For $g_{1D} < 0$, increasing the magnitude of the nonlinearity leads to the appearance of a loop structure

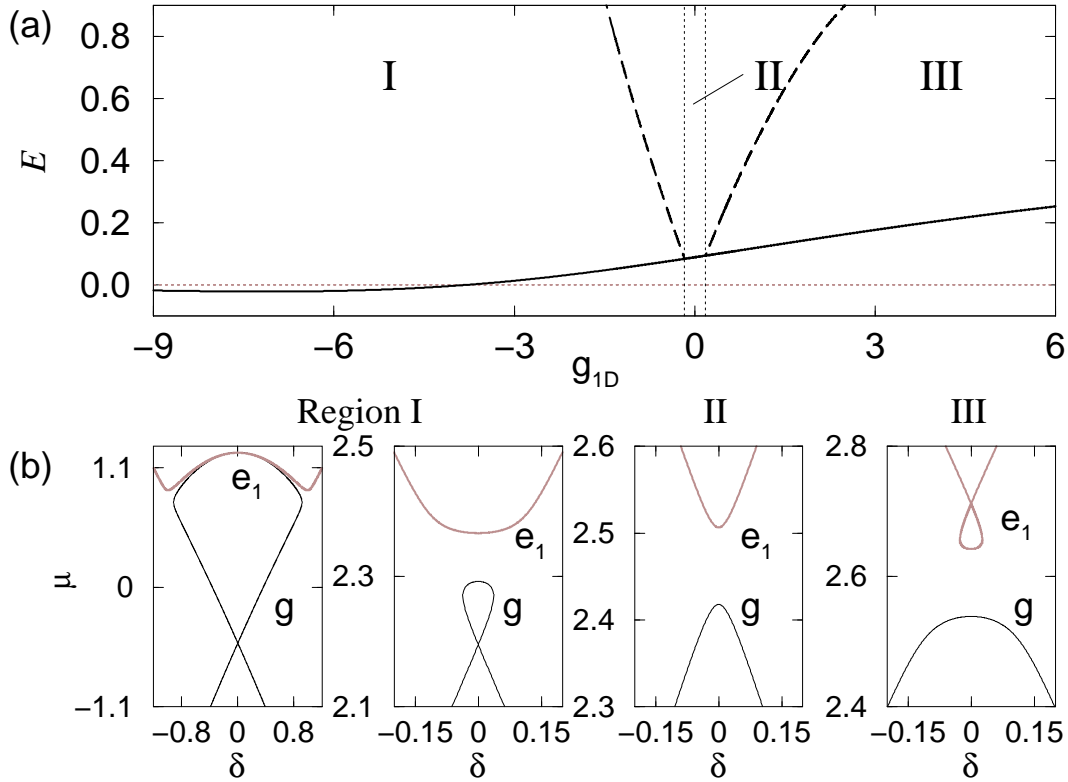


Figure 2. (a) The self-interaction energy $|E_C|$ (dashed lines) and the Josephson energy E_J (solid) at $\delta = 0$ as a function of the nonlinearity g_{1D} for the 1D confining trap with $\hbar = 4\hbar\omega_{\perp}$. (b) Typical eigenenergies μ as a function of the potential gradient δ for various nonlinearities within regions I-III. Shown are (from left to right) the cases $g_{1D} = -4, -0.5, 0$ and 0.5 . For $g_{1D} < -3.79$, $E_J < 0$. The horizontal dotted grey line corresponds to $E = 0$.

in the ground state at a critical point $|E_C| = E_J$. As a 1D condensate is stable against collapse [3, 11, 16, 25, 18, 26, 27], $|E_C|$ remains finite and a loop structure is always observed. Note that, for a nonlinearity less than a critical value, the splitting E_J becomes negative, signifying an inversion of the lowest two energy eigenvalues. This can be explained using $\mu = E - 1/2|g| \int |\Psi|^4 dr = E - |E_{\text{int}}|$. Although E is larger for the first excited state than for the ground state, the first excited state has more negative interaction energy (as its peak density is higher), thereby reducing μ below the ground state value. Fig. 2(b) shows typical eigenenergy levels for the ground and the first excited states as a function of the potential gradient for different values of the nonlinearity. The two-state model correctly reproduces the eigenenergy curves for small values of $|g_{1D}|$ but cannot reproduce the inversion of the eigenenergy levels for $g_{1D} \ll 1$. The case $g_{1D} > 0$ has been discussed in our earlier work [53].

In Fig. 3 we consider the 3D case. In Fig. 3(a) we plot the splittings $|E_C|$ and E_J at $\delta = 0$ as a function of g_{3D} . In contrast to 1D, for $g_{3D} < 0$ the condensate collapses when the atom number, or magnitude of the nonlinearity, exceeds a critical value. The

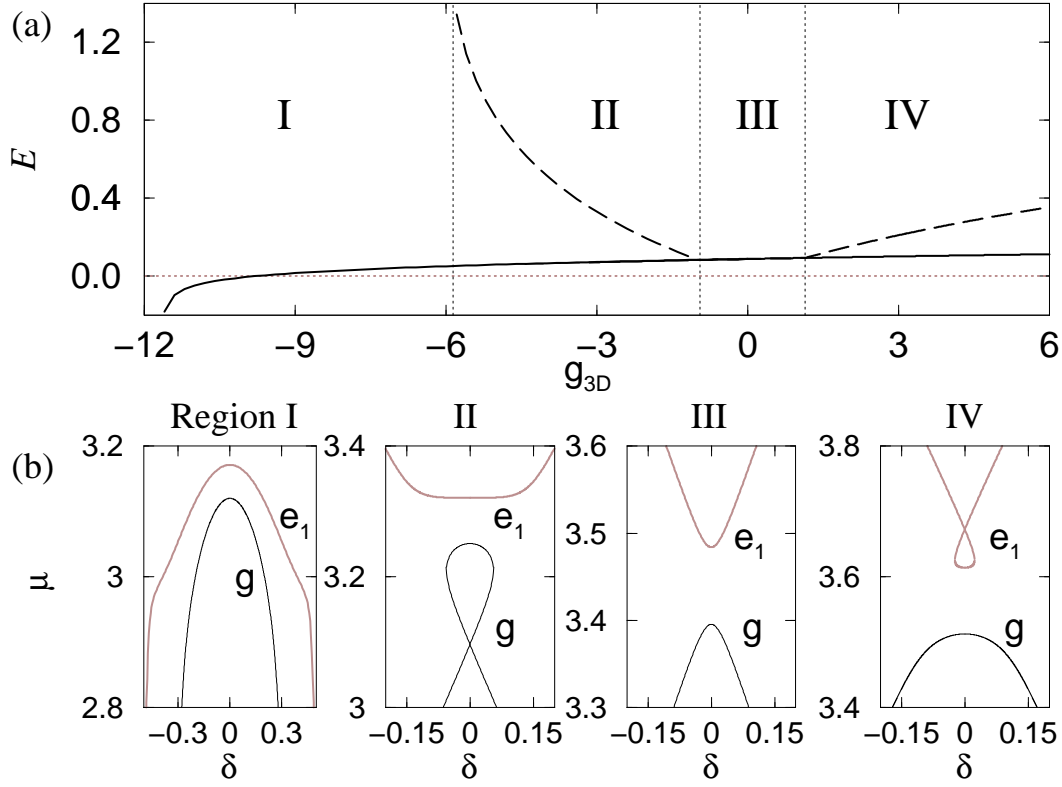


Figure 3. (a) As in Fig. 2, but for the 3D case, with $\lambda = 1$ and $h = 4\hbar\omega_{\perp}$. (b) Typical eigenenergies shown here are for each of the four regions I-IV in (a), namely (from left to right) $g_{3D} = -6, -\pi, 0$ and π . Compared to the 1D case (Fig. 2), in 3D there is an additional region (I) corresponding to the case where the self-trapped states become unstable. The horizontal dotted grey line corresponds to $E = 0$.

collapse appears first in the self-trapping states. In Fig. 3(a) this corresponds to the point where the curve for $|E_C|$ (dashed line in Fig. 3(a)) terminates at the boundary between region I and II (indicated by the vertical dotted line in Fig. 3(a)). At larger negative nonlinearities (region I in Fig. 3(a)) the lowest eigenstates invert (as in the 1D case) and at $\delta = 0$ the symmetric states also become unstable at $g_{3D} = -11.6$. In Fig. 3(b) we plot typical eigenenergy levels as a function of δ . The curves are similar to the 1D case except in the limit of large negative nonlinearities (region I), where a completely different structure is found. Note that region I cannot be described by the two-state model. In this region there is no longer a loop structure as the self trapped states are unstable. This parameter region is of interest for investigating tunnelling induced collapse, where one begins with a stable symmetric state and adds a potential gradient to induce a collapse in one well. However, before discussing the dynamical behaviour we consider the stability in the symmetric double-well as a function of the barrier height.

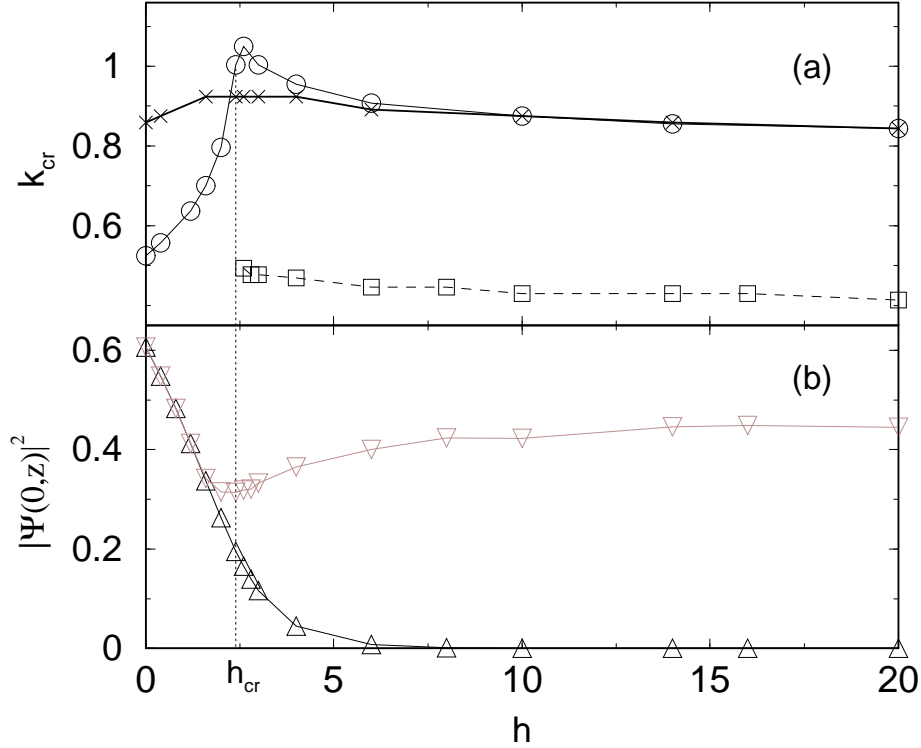


Figure 4. (a) Critical parameter k_{cr} as a function of h for a spherical geometry ($\lambda = 1$). Stability curves of the symmetric Ψ_g (curve (ii) in Fig. 1), first excited Ψ_e (curve (i)) and asymmetric ground states (iii) are shown as circles, crosses and squares respectively. (b) Condensate density $|\Psi(0, z)|^2$ along the z axis as a function of h for the state Ψ_g . Shown are the central $|\Psi(0, 0)|^2$ (black) and peak $|\Psi(0, z_m)|^2$ (grey) densities, where z_m is the longitudinal position of maximum density in the double-well configuration (i.e. centre of each individual well). In both figures, the plotted lines connect adjacent data points. The vertical dotted line highlights the critical value h_{cr} , above which the stability curve consists of two branches.

3. Stability of a 3D BEC in a double-well potential

In this Section we study the stability of a BEC with attractive interactions in a 3D symmetric double-well trap as a function of the barrier height h . We solve Eq. (1) numerically using the Newton method [53, 58]. Above the critical atom number \mathcal{N}_{cr} we no longer find stationary solutions. A dimensionless constant k_{cr} relating the scattering length a with \mathcal{N}_{cr} and the properties of the confining trap, is defined by, [11]

$$\frac{\mathcal{N}_{cr}|a|}{a_0} = k_{cr}, \quad (6)$$

where $a_0 = \sqrt{\hbar/m\omega_0}$, m is the mass of the atoms confined in the trap and $\omega_0 = \lambda^{1/3}\omega_{\perp}$ is the geometrically averaged trap frequency.

In Fig. 4(a) we plot the critical constant k_{cr} as a function of h for the case of a symmetric double-well trap with $\lambda = 1$ for the ground and first excited states. We find that at a critical value of the barrier height, h_{cr} , there are two branches to the stability

curve for the ground state. The upper and lower branches correspond to the symmetric (Fig. 1, curve (ii)) and asymmetric (Fig. 1, curve (iii)) eigensolutions respectively, (plotted by circles and squares in Fig. 4). Note also that k_{cr} reaches its maximum value at a height just above that corresponding to the appearance of the second branch. This maximum can be explained by a minimum in the peak density of the double-well configuration, which is plotted in Fig. 4(b). As the barrier is raised the condensate splits in two, thus reducing its maximum density. However, as the trap splits to form two separate condensates, the condensates in each well become compressed and the peak density increases again. Our results remain qualitatively unchanged for different values of λ . This picture is similar to that of Adhikari [55], except for the behaviour at large h , where Adhikari finds that k_{cr} increases again. As anticipated, we find that, for $h > h_{\text{cr}}$, when the system is essentially composed of two separate condensates, the value of k_{cr} in each well tends towards the value in a single harmonic trap containing the same number of atoms as each half of the double-well.

Finally, the critical constant k_{cr} as a function of h , for the first excited state, Ψ_e (crosses in Fig. 4(a)) first increases, reaches a peak value, and then decreases approaching the value for the symmetric ground state for large h . This is expected, as in the limit of large h , the density distributions of Ψ_g and Ψ_e become very similar.

4. Tunnelling Dynamics under a time-dependent magnetic field gradient

The main theme of this Section is to investigate the possibility of observing a tunnelling induced collapse. At $t < 0$ we prepare a stable condensate in a symmetric double-well, for a value of the nonlinear constant $g_{3\text{D}}$ in region I of Fig. 3(a). In order to induce a collapse, a potential gradient is applied at $t = 0$, i.e., $\delta = Rt$ for $t > 0$, such that the right well has higher potential energy than the left. Subsequently, we study the dynamics leading to the onset of collapse, by solving Eq. (1) numerically. Note that this qualitative picture should remain correct, even if 3-body loss terms are included in the treatment, although the latter may affect the precise value for the onset of the collapse.

For attractive interactions, the population difference induced by the addition of the gradient does not follow that of the eigenstate, as shown in Fig. 5(a). The effect of the nonlinearity is that the ground state is immediately projected onto a superposition of states. As the potential gradient is increased, the population in one well reaches a critical value and a collapse occurs. The critical gradient corresponding to the collapse, shown by the dotted vertical line in Fig. 5, is identified as the point where the interaction energy ($|E_{\text{int}}| = 1/2|g_{3\text{D}}| \int |\Psi|^4 dr$) diverges, see Fig. 5(b). Note that the critical value of the number asymmetry N for which the time-dependent collapse occurs is close to the maximum value of $|N_{\text{max}}|$ found for the eigensolution (grey horizontal line in Fig. 5(a)).

This prediction becomes clearer if we consider a condensate prepared in the first excited state Ψ_e , where the time evolution closely follows the eigensolution, see Fig. 5(b). In this case the collapse occurs at exactly the point where the number asymmetry

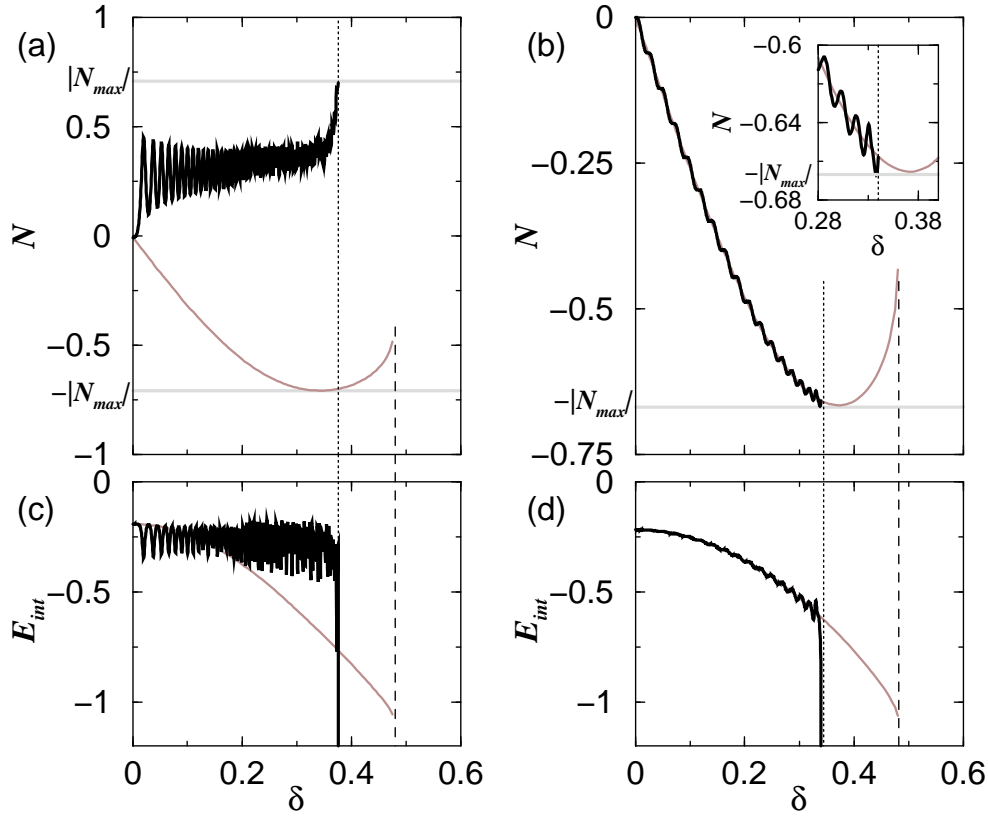


Figure 5. (a)-(b) Evolution of fractional population difference N as a function of δ for a system initially prepared in state (a) Ψ_g and (b) Ψ_e (black lines). The population difference for the eigenstates are also shown as solid grey lines. The vertical dashed lines mark the critical gradient at which the eigenstates become unstable ($\delta_0 = 0.475$ and $\delta'_0 = 0.480$ for Ψ_g and Ψ_e respectively). The vertical dotted lines describe where the system collapses in the time-dependent simulation. The collapse occurs when $|N|$ reaches the maximum value $|N_{\max}|$ (indicated by horizontal grey lines in (a) and (b)) of the number asymmetry predicted by the eigenstates. (c)-(d) Evolution of the interaction energy E_{int} (thick black line) when the potential gradient $\delta = Rt$ is increased at a constant rate R for (c) Ψ_g and (d) Ψ_e , with corresponding eigenenergies shown by grey lines. Other parameters used here: $g_{3D} = -7$, $h = 4\hbar\omega_{\perp}$, $\lambda = 1$ and $R = 10^{-3}\hbar\omega_{\perp}^2/a_{\perp}$.

exceeds $|N_{\max}|$, see inset of Fig. 5(b). The critical gradient at which the collapse is observed is found to be essentially independent of the rate R at which the gradient is increased.

One can also compare the critical number needed in one well before collapse occurs with the prediction for the symmetric potential shown in Fig. 4. By defining $K_{\text{cr}} = \mathcal{N}'_{\text{cr}}|a|/a_0$, where \mathcal{N}' is the number of atoms in the well which collapses we find that $K_{\text{cr}} = 0.471$ and 0.467 for ground and excited states in Fig. 5, which is close to the value of $k_{\text{cr}} = 0.470$ predicted by the lower branch of Fig. 4.

Finally, we discuss typical experimental parameters required for the demonstration of the tunnelling induced collapse. In the harmonic oscillator units discussed in

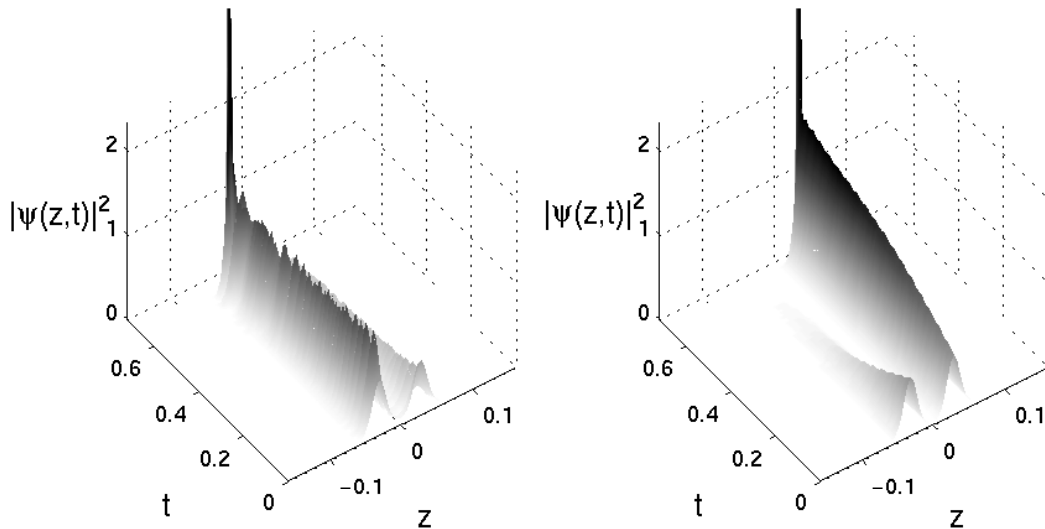


Figure 6. Surface plot of the evolution of the density distribution ($|\Psi(z,t)|^2 \times 10^{10} \text{cm}^{-3}$) along the z -axis (mm) as a function of time (s) for a BEC initially prepared in the Ψ_g (left) and Ψ_e (right) states with $g_{3D} = -6$. Due to the potential gradient, tunnelling is induced to the left ($z < 0$) well for the Ψ_g state and to the right well for Ψ_e . The condensate instability occurs at $t = 0.65$ s for Ψ_g and 0.67 s for Ψ_e . Other parameters as in Fig. 5.

Section 2, the number of atoms is given by,

$$\mathcal{N} = \frac{g_{3D}}{4\pi} \frac{a_{\perp}}{a} = \frac{g_{3D}}{4\pi a} \sqrt{\frac{\hbar}{m\omega_{\perp}}} . \quad (7)$$

For ^7Li atoms and taking $g_{3D} = -6$ and $\omega_{\perp} = 2\pi \times 100$ Hz, we find $\mathcal{N} = 1200$ which is below the critical value for collapse. For an applied field gradient $R = (10^{-3})(\hbar\omega_{\perp}/a_{\perp})$ the collapse occurs at $t_{\text{exp}} \sim 0.6$ s. The collapse is illustrated by the density plots shown in Fig. 6. We have confirmed that the collapse can be avoided if the potential gradient is ramped up to a value smaller than the critical gradient and then held constant. This would not hold if the system were very close to the critical region, in which case number fluctuations [59, 60] could enhance tunnelling and hence induce the collapse at a slightly smaller gradient than that predicted by our simple model.

5. Conclusions

We have studied the stability of a low temperature atomic BEC with attractive interactions in a 1D and 3D double-well potential. In particular we highlight a regime where the condensate is stable if the population in both wells are approximately equal, but becomes unstable if there is sufficient tunnelling from one well to the other. We study the dynamics of the system when driven by a time-dependent potential gradient and show that a collapse occurs at a critical gradient predicted by the time-independent solutions. Although this picture is expected to be qualitatively correct in low temperature atomic condensates, further work is required to determine the precise

details of the onset of collapse and the subsequent collapse dynamics, as well as the effects of fluctuations [59, 60] and finite temperature [61, 62].

Acknowledgments

We acknowledge funding from the UK EPSRC.

References

- [1] Anderson M H, Ensher J R, Mathews M R, Wieman C E, and Cornell E A, *Science* **269**, 198 (1995)
- [2] Davis K B, Mewes M -O, Andrews M R, van Druten N J, Durfee D S, Kurn D M, and Ketterle W, *Phys. Rev. Lett.* **75**, 3969 (1995)
- [3] Bradley C C, Sackett C A, Tollett J J, and Hulet R G, *Phys. Rev. Lett.* **75**, 1687 (1995); Bradley C C, Sackett C A, and Hulet R G, *Phys. Rev. Lett.* **78**, 985 (1997)
- [4] Fried D G, Killian T C, Willmann L, Landhuis D, Moss S C, kleppner D, and Greytak T J, *Phys. Rev. Lett.* **81**, 3811 (1998)
- [5] Robert A, Sirjean O, Browaeys A, Poupard J, Nowak S, Boiron D, Westbrook C I, and Aspect A, *Science* **292**, 461 (2001)
- [6] Cornish S L, Claussen N R, Roberts J L, Cornell E A and Wieman C E, *Phys. Rev. Lett.* **85**, 1795 (2000)
- [7] Modugno G, Ferrari G, Roati G, Brecha R J, Simoni A, and Inguscio M, *Science* **294**, 1320 (2001)
- [8] Weber T, Herbig J, Mark M, Nagerl H -C, and Grimm R, *Science* **299**, 232 (2003)
- [9] Takasu Y, Maki K, komori K, Takano T, Honda K, Kumakura M, Yabuzaki T, and Takahashi Y, *Phys. Rev. Lett.* **91**, 040404 (2003)
- [10] Tiesinga E, Verhaar B J, and Stoof H T C, *Phys. Rev. A* **47**, 4114 (1993); Courteille P, Freeland R S, Heinzen D J, van Abeelen F A, and Verhaar B J, *Phys. Rev. Lett.* **81**, 69 (1998); Inouye S, Andrews M R, Stenger J, Miesner H -J, Stamper-Kurn D M and Ketterle W, *Nature* **392**, 151 (1998)
- [11] Ruprecht P A, Holland M J, Burnett K, and Edwards M, *Phys. Rev. A* **51**, 4704 (1995)
- [12] Dodd R J, Edwards M, Williams C J, Clark C W, Holland M J, Ruprecht P A and Burnett K, *Phys. Rev. A* **54**, 661 (1996)
- [13] Houbiers M and Stoof H T C, *Phys. Rev. A* **54**, 5055 (1996)
- [14] Pitaevskii L P, *Phys. Lett. A* **221**, 14 (1996)
- [15] Kagan Yu, Shlyapnikov G V and Walraven J T M, *Phys. Rev. Lett.* **76**, 2670 (1996)
- [16] Shuryak E V, *Phys. Rev. A* **54**, 3151 (1996)
- [17] Dalfovo F and Stringari S, *Phys. Rev. A* **53**, 2477 (1996)
- [18] Dalfovo F, Giorgini S, Pitaevskii L P, and Stringari S, *Rev. Mod. Phys.* **71**, 463 (1999)
- [19] Stoof H T C, *J. Stat. Phys.* **87**, 1353 (1997)
- [20] Perez-Garcia V M, Michinel H, Cirac J I, Lewenstein M and Zoller P, *Phys. Rev. A* **56**, 1424 (1997)
- [21] Shi H and Zheng W-M, *Phys. Rev. A* **55**, 2930 (1997)
- [22] Fetter A L, *J. Low Temp. Phys.* **106**, 643 (1997)
- [23] Ueda M and Leggett A J, *Phys. Rev. Lett.* **80**, 1576 (1998)
- [24] Parola A L, Salasnich L and Reatto L, *Phys. Rev. A* **57**, R3180 (1998)

- [25] Kagan Y, Muryshv A E, and Shlyapnikov G V, Phys. Rev. Lett. **81**, 933 (1998)
- [26] Eleftheriou E and Huang K, Phys. Rev. A **61**, 043601 (2000)
- [27] Adhikari S K, Phys. Rev. E **65**, 016703 (2002)
- [28] Gammal A, Frederico T and Tomio L, Phys. Rev. A **64**, 055602 (2001); Gammal A, Tomio L and Frederico T, Phys. Rev. A **66**, 043619 (2002)
- [29] Sackett C A, Stoof H T C, and Hulet R G, Phys. Rev. Lett. **80**, 2031 (1998)
- [30] Sackett C A, Gerton J M, Welling M, and Hulet R G, Phys. Rev. Lett. **82**, 876 (1999)
- [31] Strecker K E, Partridge G B, Truscott A G, and Hulet R G, Nature **417**, 150 (2002); Al Khawaja U, Stoof H T C, Hulet R G, Strecker K E, and Partridge G B, Phys. Rev. Lett. **89**, 200404 (2002)
- [32] Donley E A, Claussen N R, Cornish S L, Roberts J L, Cornell E A, and Wieman C E, Nature **412**, 295 (2001); Roberts J L, Claussen N R, Cornish S L, Donley E A, Cornell E A, and Wieman C E, Phys. Rev. Lett. **86**, 4211 (2001)
- [33] Duine R A and Stoof H T C, Phys. Rev. Lett. **86**, 2204 (2001)
- [34] Adhikari S K, Phys. Rev. A **66**, 013611 (2002); S. K. Adhikari, Phys. Rev. A **66**, 043601 (2002)
- [35] Santos L and Shlyapnikov G V, Phys. Rev. A **66**, 011602 (2002)
- [36] Saito H and Ueda M, Phys. Rev. A **65**, 033624 (2002)
- [37] Savage C M, Robins N P and Hope J J, Phys. Rev. A **67**, 014304 (2003)
- [38] Milstein J N, Menotti C, and Holland M J, New J. Phys. **5**, 52 (2003)
- [39] Adhikari S K, J. Phys. B: At. Mol. Opt. Phys. **37**, 1185 (2004)
- [40] Bao W, Jaksch D, and Markowich P A, J. Phys. B: At. Mol. Opt. Phys. **37**, 329 (2004)
- [41] Andrews M R, Townsend C G, Miesner H J, Durfee D S, Kurn D M and Ketterle W 1997 Science **275** 637
- [42] Tiecke T G, Kemmann M, Buggle C, Shvarchuck I, von Klitzing W and Walraven J T M, J. Opt. B: Quantum Semiclass. Opt. **5**, S119 (2003)
- [43] Shin Y, Saba M, Pasquini T A, Ketterle W, Pritchard D E, and Leanhardt A E, 2004 Phys. Rev. Lett. **92**, 050405
- [44] Shin Y, Saba M, Schirotzek A, Pasquini T A, Leanhardt A E, Pritchard D E, and Ketterle W, Phys. Rev. Lett. **92**, 150401 (2004)
- [45] Thomas N R and Wilson A C, Foot C J, 2002 Phys. Rev. A **65**, 063406
- [46] Jack M W, Collett M J and Walls D F, Phys. Rev. A **54**, R4625 (1996)
- [47] Smerzi A, Fantoni S, Giovanazzi S and Shenoy S R 1997 Phys. Rev. Lett. **79** 4950
- [48] Raghavan S, Smerzi A, Fantoni S, and Shenoy S R 1999 Phys. Rev. A **59** 620
- [49] Zapata I, Sols F and Leggett A 1998 Phys. Rev. A **57** R28
- [50] Wu B and Niu Q 2000 Phys. Rev. A **61** 023402
- [51] Williams J 2001 Phys. Rev. A **64** 013610
- [52] Giovanazzi S, Smerzi A and Fantoni S 2000 Phys. Rev. Lett. **84** 4521
- [53] Sakellari E, Leadbeater M, Kylstra N J and Adams C S 2002 Phys. Rev. A **66** 033612
- [54] Sakellari E, Proukakis N P, Leadbeater M, and Adams C S 2004 New J. Phys. **6** 94
- [55] Adhikari S K, J. Phys. B: At. Mol. Opt. Phys. **36**, 2943 (2003)
- [56] Couillet P and Vandenbergh, J. Phys. B: At. Mol. Opt. Phys. **35**, 1593 (2002)
- [57] Wu B, Diener R B and Niu Q 2002 Phys. Rev. A **65** 025601
Diakonov D, Jensen L M, Pethick C J and Smith H 2002 Phys. Rev. A **66** 013604
Mueller E J 2002 Phys. Rev. A **66** 063603
- [58] Press W H, Teukolsky S A, Vetterling W T and Flannary B P, *Numerical recipes in FORTRAN : the art of scientific computing* 2nd Ed. CUP, Cambridge, 1992.
- [59] Leggett A J and Sols F 1991 Found. Phys. **21**, 353.
- [60] Javaneinen J and Ivanov M Yu 1999 Phys. Rev. A **60**, 2351.
- [61] Ruostekoski J and Walls D F 1998 Phys. Rev. A **58**, R50.
- [62] Zapata I, Sols F and Leggett A J 1998 Phys. Rev. A **57**, R28.